Brain (1999), **122,** 1085–1092

Mutant channels contribute <50% to Na^+ current in paramyotonia congenita muscle

Nenad Mitrovic,[1,3] Alfred L. George Jr,[4] Reinhardt Rüdel,[2] Frank Lehmann-Horn[1] and Holger Lerche[1,3]

Departments of [1]Applied and [2]General Physiology and [3]Neurology, University of Ulm, Germany and [4]Departments of Medicine and Pharmacology, Vanderbilt University, Nashville, Tenn., USA

Correspondence to: Dr Nenad Mitrovic, Department of Applied Physiology/Neurology, University of Ulm, D-89069 Ulm, Germany
E-mail: nenad.mitrovic@medizin.uni-ulm.de

Summary

An important question in the pathophysiology of dominantly inherited diseases, such as channelopathies, is the level of expression of the mutant protein. In our study, we address this issue by comparing the gating defects of two human muscle Na^+ channel mutants (R1448C and R1448P) causing paramyotonia congenita in native muscle specimens from two patients with those of the same mutant recombinant channels expressed in human embryonic kidney (HEK-293) cells. Patch-clamp recordings of transfected HEK-293 cells revealed a pronounced slowing of the Na^+ current decay, a left-shifted and decreased voltage dependence of steady-state inactivation, and an increased frequency of channel reopenings for mutant compared with wild-type channels. For R1448P channels, inactivation was almost six-fold and for R1448C it was three-fold slower than for wild-type channels. The same defects, though less pronounced, as expected for a disorder with dominant inheritance, were observed for muscle specimens from paramyotonia congenita patients carrying these mutations. Quantitative kinetic analysis of Na^+ channel inactivation in the paramyotonic muscle specimens separating wild-type from mutant channels suggested that no more than 38% of the channels in the paramyotonia congenita muscle specimen were of the mutant type. Our data raise the possibility that variability in the ratio of mutant to wild-type Na^+ channels in the muscle membrane has an impact on the clinical severity of the phenotype.

Keywords: Na^+ channel; inactivation; channelopathies; patch-clamp; human skeletal muscle

Abbreviation: I_{SS}/I_{PEAK} = relative persistent Na^+ current

Introduction

Paramyotonia congenita is a dominantly inherited muscle disorder characterized by paradoxical myotonia, which is muscle stiffness increasing with repeated activity, and weakness triggered by exposure to cold. Stiffness and weakness are caused by an unstable muscle fibre membrane potential. EMG recordings show long-lasting series of action potentials during muscle effort or electrical silence during periods of paralysis.

Normal excitability of muscle fibres requires a high resting potential and short-lasting action potentials. Neither requirement is fulfilled in paramyotonia congenita, as shown with microelectrode recordings on excised muscle from patients. Voltage-clamp studies of single fibres have revealed that inactivation of Na^+ currents is incomplete (Lehmann-Horn *et al*., 1987).

Recently, we applied the patch-clamp technique to blebs of muscle fibres from a paramyotonia congenita patient carrying the arginine-1448-proline (R1448P) mutation within the voltage sensor IV/S4 of the α-subunit of the human skeletal muscle Na^+ channel (Lerche *et al*., 1996). The major abnormal findings were that (i) the defective channels tend to reopen spontaneously after a 'physiological' opening upon depolarization and (ii) the sum of responses from many channels showed a much slower Na^+ current decay. These reopenings increase Na^+ influx into the muscle fibres, causing either slight depolarization with hyperexcitability (myotonia) or substantial depolarization with inexcitability (paralysis) of the muscle.

About 20 different disease-causing mutations have been found in the gene encoding the α-subunit of the adult skeletal muscle Na^+ channel, six of them resulting in paramyotonia congenita [the others cause either hyperkalaemic periodic paralysis or potassium-aggravated myotonia, reviewed by Lehmann-Horn and Rudel (Lehmann-Horn and Rudel, 1996)]. The electrophysiological properties of an ion channel can be elegantly examined by expressing the recombinant channel

DNA in cultivated cells. Advantages are that (i) the Na^+ channel population is homogeneously wild type or mutant and (ii) muscle biopsy is not required. Direct comparison of wild-type and mutant channels in both natural and artificial milieus has not been performed. Here, we provide a detailed analysis of the R1448P mutation, which has not been expressed in human embryonic kidney (HEK-293) cells before and we compare two mutations causing paramyotonia congenita (R1448C and R1448P) in both expression systems—native muscle of paramyotonia congenita patients and HEK-293 cells. A quantitative analysis of Na^+ channel inactivation kinetics allowed us to estimate that in the patient's muscle the mutant channels contribute only 20–38% of the Na^+ current, less than expected for a disease with a dominant mode of inheritance.

Material and methods

The arginine-1448-cysteine/proline mutations were created by site-directed mutagenesis using the Altered Sites system (Promega Corporation, Madison, Wis., USA) as described (Chahine *et al*., 1994). Wild-type and mutant constructs were assembled in the mammalian expression vector pRC/CMV and transfected into human embryonic kidney cells (HEK-293) by the calcium phosphate precipitation method. Stable cell lines expressing either wild-type or mutant channels were obtained by antibiotic selection as described (Mitrovic *et al.*, 1994).

Standard whole-cell recordings were performed using an EPC-7 amplifier (List, Darmstadt, Germany). The voltage error due to series resistance was <5 mV. Leakage and capacitative currents were subtracted automatically by a prepulse protocol (–P/4). All data were filtered with 3 kHz and digitized at 20 kHz using pClamp 6.02 (Axon Instruments, Foster City, Calif., USA). Analysis was based on pClamp, Excel 97 (Microsoft, Redmond, Mass., USA), Origin 5.0 (Microcal Software, Northampton, Mass., USA), Sigma Plot 5.0 (Jandel Scientific, San Rafael, Calif., USA) and our own software. The solutions were as follows (in mM, pH 7.4). Whole-cell recordings: pipette: 135 CsCl, 5 NaCl, 2 $MgCl_2$, 5 EGTA and 10 HEPES; bath: 140 NaCl, 4 KCl, 2 $CaCl_2$, 1 $MgCl_2$, 4 dextrose and 5 HEPES. Single channels were recorded in the cell-attached configuration using the following solutions: pipette: 150 NaCl, 4 KCl, 2 $CaCl_2$, 1 $MgCl_2$, 10 TEACl and 10 HEPES; bath: 150 KCl, 5 NaCl, 2 $CaCl_2$, 1 $MgCl_2$ and 10 HEPES. Recordings from sarcolemmal blebs of native muscle were performed in the bleb-attached mode as described by Lerche and colleagues (Lerch *et al*., 1996). Biopsy was performed under local anaesthesia from the quadriceps muscle with informed consent of the patient, as described by Lerche and colleagues (Lerche *et al*., 1996). All procedures were in accordance with the Helsinki convention and were approved by the Ethical Committee of the University of Ulm. Experiments were performed at 21°–22°C if not stated otherwise. The temperature was controlled via a water-perfused Petri dish holder. For statistical evaluation, Student's *t* test was applied. All data are shown as mean ± standard error of the mean.

Results and discussion

Voltage-gated Na^+ channels are the basis for the generation and conduction of action potentials in nerve and muscle cells. They open briefly upon depolarization and then close to a fast inactivated state from which they reopen very rarely. Thus fast inactivation limits the duration of an action potential and initiates its repolarizing phase. The muscle membrane becomes inexcitable for a short period of time after an action potential; this is the so-called refractory period. This time is determined by the recovery of the Na^+ channel from inactivation. Thus, recovery from inactivation limits the firing rate of nerve and muscle cells. These characteristics of Na^+ channels can be determined electrophysiologically using the patch-clamp technique. By comparison of the mutant with the wild-type phenotype, gating defects can be elucidated in detail.

Whole-cell recordings of Na^+ currents through R1448P channels in HEK-293 cells

The R1448P mutation results in the substitution of a neutral proline for a positively charged arginine in the S4 segment of domain IV of the Na^+ channel α-subunit, which is composed of four highly homologous domains containing six transmembrane segments each (for review, see Catterall, 1995). Positively charged residues in S4 segments constitute the Na^+ channel voltage sensor and play a central role in Na^+ channel gating (for review, see Horn, 1999). Families of Na^+ currents for wild-type and R1448P channels are shown in Fig. 1A and B. Currents of the mutant channels decayed much more slowly than those of the wild type, indicating impaired channel inactivation. The current decay was best fitted with the sum of two exponentials, yielding two inactivation time constants (τ_{h1} and τ_{h2}). With respect to wild type, for R1448P the faster time constant τ_{h1} (relative weight $>75\%$) was almost sixfold larger at a test potential of 0 mV (Fig. 3B).

The persistent Na^+ current (I_{SS}) represents the proportion of non-inactivating channels. We have shown previously that I_{SS} may cause a sustained membrane depolarization in paramyotonia congenita muscle fibres, resulting in the clinical symptom of paralysis (Lehmann-Horn *et al.*, 1987; Lerche *et al*., 1996). Therefore, we determined a persistent current at the end of a depolarizing test pulse and normalized it to the peak current (I_{PEAK}). It was increased 1.5-fold in R1448P channels compared with wild-type channels (Fig. 1C).

For R1448P channels, the steady-state activation curve describing the voltage dependence of channel opening was shifted by –8 mV (Fig. 1D). This shift might represent a real alteration of the activation process, but could also reflect the

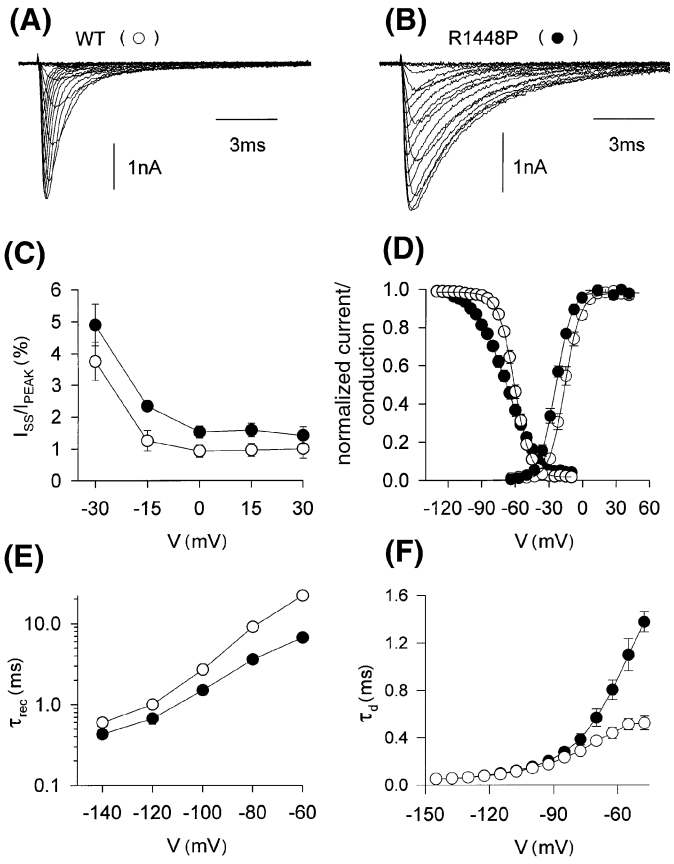

Fig. 1 Gating of R1448P Na^+ channels expressed in HEK cells. (**A**, **B**) Current traces from whole-cell recordings of wild-type (WT) and R1448P mutant Na^+ channels. Cells were held at –85 mV and depolarized for 100 ms to various test potentials (see abscissa in **D**) after a 300-ms prepulse to –120 mV. Note persistent currents in **B**. (**C**) The persistent Na^+ current normalized to the initial peak current, evaluated from 100-ms traces as described in the legend to Fig. 3. I_{SS}/I_{PEAK} at 0 mV, 0.87 ± 0.20 versus 1.53 ± 0.19%, n = 9–10, $P < 0.05$. (**D**) Steady-state activation and inactivation curves. Steady-state inactivation was determined with 300-ms prepulses to the indicated potentials prior to the 4-ms test pulse to 0 mV (–85 mV holding potential). Lines represent fits to standard Boltzmann functions ($I/I_{MAX} = 1/[1 + \exp([V - V_{0.5}]/k)]$) with the following parameters (wild type versus R1448P in mV): activation: $V_{0.5}$ = –16 ± 1 versus –24 ± 1 ($P < 0.001$), slope k = –5.9 ± 0.3 versus –7.1 ± 0.3 ($P < 0.01$), n = 8–10; inactivation: $V_{0.5}$ = –61 ± 1 versus –68 ± 2 ($P < 0.05$), k = 6.6 ± 0.2 versus 13.6 ± 0.5 ($P < 0.0001$), n = 8–9. (**E**) Voltage dependence of recovery from inactivation. Cells were held at –100 mV, prepulsed to 0 mV for 100 ms to inactivate all Na^+ channels and repolarized to the recovery potential for increasing durations prior to the test pulse to 0 mV. At –60 and –80 mV, the time course of recovery was best fitted with a single exponential, at –100, –120 and –140 mV with a sum of two exponentials (with relative amplitudes of the second slower component between 10 and 30%). Values of τ_{rec1} in ms for wild type versus R1448P at –60 and –100 mV: 22.1 ± 1.2 versus 6.7 ± 0.6 ($P < 0.0001$), 2.7 ± 0.2 versus 1.5 ± 0.2 ($P < 0.01$). (**F**) Deactivation determined at 15°C, by a 0.6 ms activating pulse to +20 mV followed by the test pulse to the indicated potentials. The deactivation time constant, τ_d, was obtained by fitting an exponential to the current decay. There was no significant difference between wild-type and mutant channels at potentials more negative than –90 mV.

influence of the slowed inactivation on our procedure for determining the activation curve: all currents were normalized to the largest peak current, which was delayed in R1448P. The steady-state inactivation curve, representing the proportion of non-inactivated Na^+ channels, was shifted by –7 mV and its slope was markedly reduced (Fig. 1D). These changes have two important implications with regard to the weakness in paramyotonia congenita: (i) at the resting potential, the number of Na^+ channels available for an action potential is markedly reduced (at –80 mV only 60% of mutant channels versus 95% of wild-type channels), and (ii) at less negative potentials the increased overlap of the activation and inactivation curves creates a larger permanent 'window' current. The first point directly reduces excitability; the second furthers depolarization, i.e. it also reduces excitability.

Recovery from inactivation was significantly accelerated and its voltage dependence decreased for R1448P (Fig. 1E). The faster recovery from inactivation, which was also found for several other paramyotonia congenita or potassium-aggravated myotonia-causing mutations (Chahine *et al*., 1994; Yang *et al*., 1994; Mitrovic *et al*., 1994), promotes the development of myotonia by shortening the refractory period after an action potential.

The tail current decay describes Na^+ channel deactivation, the closing of open channels upon membrane repolarization. For some mutations causing potassium-aggravated myotonia (Mitrovic *et al*., 1995) but also for the R1448P mutation (Featherstone *et al*., 1998), it has been proposed that slowed deactivation increases the Na^+ inward current and may therefore contribute to membrane depolarization and myotonia. In our study, the deactivation time constants were identical for both channel types in the voltage range where no inactivation occurred (Fig. 1F), suggesting normal deactivation for R1448P.

In summary, R1448P affects inactivation and recovery from inactivation with minor effects on activation. Recent studies have shown that S4 segments in Na^+ channels are specialized in their function. Whereas S4s in the first three domains play a more important role in activation, the S4 segment of the fourth domain seems to serve a double duty, but a more important one in inactivation (Stuhmer *et al*., 1989; Chahine *et al*., 1994; Chen *et al*., 1996; Yang *et al*., 1996; Mitrovic *et al*., 1998).

The electrophysiological phenotype of R1448C channels has been described in detail before (Chahine *et al*., 1994). We would like to summarize the most important gating differences from wild-type and R1448P channels found in our study, which is important in the light of the comparison of native channels with those expressed in HEK cells, since these experiments were performed with both the R1448P and the R1448C mutation. R1448C channels were expressed, measured and analysed in the same way as described above for wild-type and R1448P channels. The fast inactivation time constant, τ_{h1}, was 1.46 ± 0.08 ms at 0 mV, thus only threefold higher than that for the wild type, whereas R1448P channels showed a 5.8-fold increase in τ_{h1}. The negative

shift of steady-state inactivation was more pronounced for R1448C than for R1448P channels ($V_{0.5}$ = –79 ± 2 mV for R1448C), while the steepness was not decreased as much for R1448C (k = 11.4 ± 0.3 mV). Steady-state activation was slightly shifted towards more negative potentials, and recovery from inactivation was accelerated for R1448C compared with wild type, as has been described previously (Chahine *et al.*, 1994).

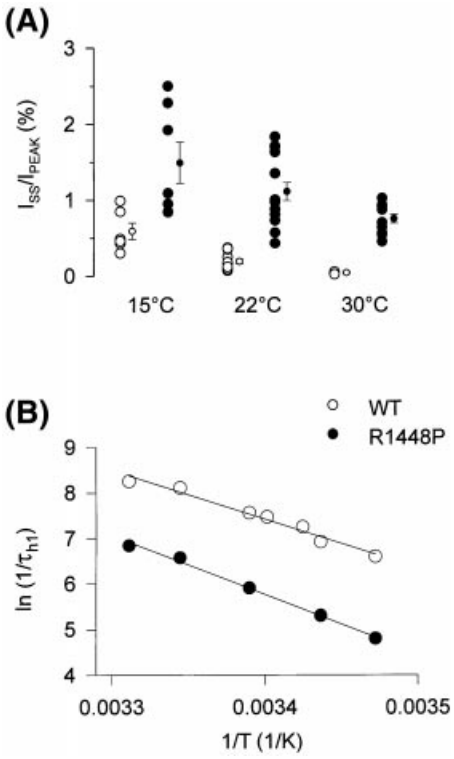

Fig. 2 Effects of temperature. (**A**) Frequency of late channel reopenings, occurring between 90 and 190 ms after the onset of depolarization, in relation to the average initial peak current determined from single-channel recordings from HEK cells at 15°, 22° and 30°C. At least 300 traces from patches containing up to 100 Na^+ channels were evaluated. The I_{SS}/I_{PEAK} was significantly increased for R1448P at all temperatures investigated (at 22°C, 0.19 ± 0.03 versus 1.11 ± 0.12%, n = 13–14, $P < 0.001$). (**B**) Arrhenius plot for τ_{h1} obtained from whole-cell recordings at different temperatures, indicating a similar temperature sensitivity for wild-type (WT) and mutant channels (E_a = 21.2 ± 1.6 versus 24.7 ± 1.6 kcal/mol).

Single-channel studies and the effects of temperature

The slowing of inactivation and the increased persistent current could be due to an increased frequency of reopenings, to prolonged openings and/or later first openings of the mutant channels. To discriminate between these possibilities, we recorded single-channel currents using test pulses from a holding potential of –120 mV to –30 mV. First latencies were similar (0.6 ± 0.1 versus 0.7 ± 0.1 ms in wild type, n = 3–4) and mean open times were slightly prolonged for R1448P compared with wild-type channels. The mean open time histograms were best fitted with the sum of two exponentials. The respective time constants for R1448P and wild type were τ_1 = 0.26 ± 0.02 and 0.19 ± 0.01 ms ($P <$ 0.01), τ_2 = 0.97 ± 0.06 and 0.83 ± 0.10 ms ($P > 0.05$); relative weights of τ_2 were 50 ± 3 and 25 ± 4% ($P <$ 0.001) (n = 8–13). Normalized late Na^+ currents calculated from reopenings were significantly increased in R1448P (Fig. 2A), corresponding to the larger persistent current in macroscopic recordings.

Since the symptoms of paramyotonia congenita are aggravated by cold, we evaluated the effects of temperature on the kinetics of Na^+ channel inactivation and on late Na^+ currents in the range from 15° to 30°C. Slower current decay and increased persistent current were seen over the whole temperature range for R1448P channels (Fig. 2A and B). The temperature sensitivity was determined as the activation energy E_a from Arrhenius plots for τ_{h1}. The value of E_a was not increased for R1448P channels (Fig. 2B). These data suggest that it is not an increased temperature dependence of mutant channels that underlies the sensitivity to cold in paramyotonia congenita, as has also been found for several other paramyotonia congenita mutations (Chahine *et al.*, 1994; Yang *et al*., 1994; Hayward *et al*., 1996; Fleischhauer *et al*., 1998). We therefore propose that a certain threshold of inactivation failure has to be exceeded in a cold environment to induce myotonia and/or paralysis.

Pathophysiology of paramyotonia congenita

One of the key symptoms in paramyotonia congenita is paradoxical myotonia, muscle stiffness increasing with continued activity, which is in contrast to the 'warm-up' phenomenon seen with the chloride channel myotonias Thomsen and Becker. Paramyotonia congenita-causing mutations result predominantly in a slowing of fast inactivation (Chahine *et al*., 1994; Yang *et al*., 1994; Hayward *et al*., 1996), which is most pronounced in R1448P. The slowed current decay provides a plausible explanation for paradoxical myotonia since in this case continued exercise would result in the accumulation of intracellular Na^+ and muscle depolarization.

Previous studies on paramyotonia congenita muscle fibres have shown that paralysis is caused by increased Na^+ influx depolarizing the muscle fibres to –40 mV and rendering them inexcitable (Lehmann-Horn *et al*., 1987; Lerche *et al*., 1996). With regard to our electrophysiological results, we propose that a combination of an increased persistent current, exceeding a certain threshold in the cold, and the left-shift of steady-state inactivation cause weakness and paralysis in paramyotonia congenita.

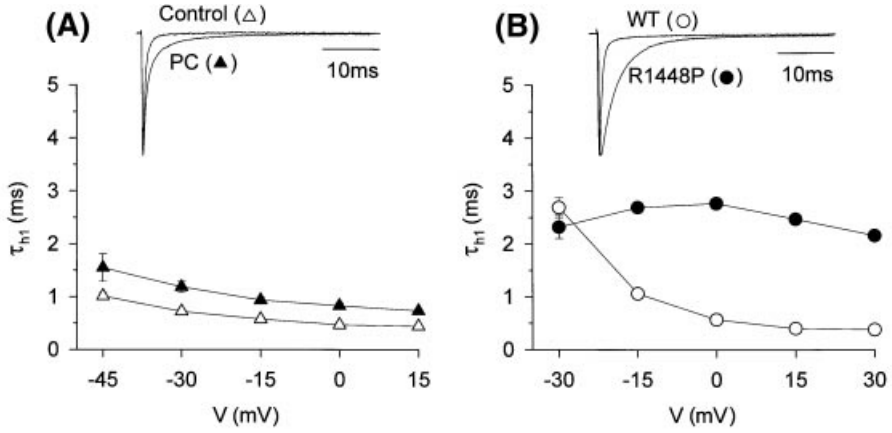

Fig. 3 Comparison of native and heterologously expressed Na^+ channels. Fast inactivation time constants, τ_{h1}, for Na^+ currents recorded from a control and a paramyotonia congenita muscle from a patient carrying the R1448P mutation (**A**) and from wild-type (WT) and R1448P channels expressed in HEK-293 cells (**B**). The insets show normalized, superimposed, representative current traces elicited by test pulses to –15 mV (muscle) and 0 mV (HEK cells). Data in **A** have been published previously (Lerche *et al.*, 1996). For both expression systems, the time course of inactivation was well fitted by the sum of two exponentials: $I/I_{PEAK} = A_1\exp(-t/\tau_{h1}) + A_2\exp(-t/\tau_{h2}) + I_{SS}/I_{PEAK}$. The value of τ_{h1} was 1.6-fold larger in paramyotonia congenita (PC) than in control muscle (at –15 mV, 0.93 ± 0.05 versus 0.57 ± 0.03 ms, $n = 7$–16, $P < 0.001$, [2]). The value of τ_{h1} in HEK cells was increased 5.8-fold for R1448P compared with wild type (at 0 mV, 2.77 ± 0.11 versus 0.48 ± 0.01 ms, $n = 10$–16, $P < 0.0001$).

Comparison of currents through mutant channels in HEK-293 cells and in paramyotonia congenita muscle

Inactivation was more slowed in HEK cells than in the paramyotonia congenita muscle (Fig. 3) because the former contain 100% mutant channels, whereas the muscle should contain 50% according to dominant inheritance. To pursue our main aim, i.e. to calculate the percentage of mutant channels in muscle from patients carrying the R1448P or R1448C mutations, we analysed and compared the decay of the Na^+ currents in HEK cells and in muscle. This approach was justified because the properties of wild-type channels were very similar in the two expression systems. In both systems, the current decay of wild-type channels was well fitted to a second-order exponential function with a major fast time constant τ_{h1} (relative weight > 90%) only slightly prolonged in muscle (0.48 ± 0.01 ms at 0 mV in HEK cells and 0.57 ± 0.03 ms at –15 mV in muscle). We compared a test potential of 0 mV in HEK cells with –15 mV in muscle since the I–V curve was shifted by –15 mV and peaked at these potentials [the steady-state activation and inactivation curves were shifted in the hyperpolarizing direction by –15 and –30 mV, respectively, most probably owing to giga-seal formation in cell-attached patches (Fahlke and Rudel, 1992)].

Previously, we compared Na^+ channels in muscle from a paramyotonia congenita patient carrying the R1448P mutation and from normal controls by fitting the current decay to a second-order exponential function (Lerche *et al.*, 1996; Fig. 3A). The largest difference between paramyotonia congenita and control was a 1.6-fold increase in τ_{h1} (0.57 ± 0.03 and 0.93 ± 0.05 ms; $n = 7$–15). In contrast, in HEK cells the most pronounced difference was a 5.8-fold increase in τ_{h1} for R1448P compared with wild-type channels (Fig. 3B; τ_{h1} at 0 mV, 0.48 ± 0.01 and 2.77 ± 0.11 ms; $n = 10$–16). This result already suggests that the percentage of mutant channels in the paramyotonia congenita muscle specimen is less than 50%. Compared with the drastic changes in the major fast inactivation time constant, differences in τ_{h2} and its relative weight were small, or at least that their contribution to the slowing of the current decay was not large (values in native control versus paramyotonia congenita muscle at –15 mV: τ_{h2}, 6.2 ± 0.4 versus 7.2 ± 1.0 ms; A_2, 6.8 ± 0.9 versus 23.3 ± 1.9%; values in HEK cells for wild type versus R1448P channels at 0 mV: τ_{h2}, 8.1 ± 1.3 versus 12.2 ± 2.1 ms; A_2, 3.3 ± 0.5 versus 18.5 ± 2.9%).

In order to separate the different time constants deriving from mutant and wild-type channels in paramyotonia congenita muscle, we fitted multiple exponentials to the current decay at –15 mV. Theoretically, there should be four different time constants of inactivation, i.e. τ_{h1} and τ_{h2} for both wild-type and mutant channels. However, it was not possible to separate the two slow time constants because their amplitudes were too small and their difference was only marginal (see above). Three time constants could be well separated. We concluded that the shortest time constant represented the fast inactivation component of the wild-type channels: the intermediate time constant represented the fast inactivation component of the mutant channels and the slowest time constant represented the slow inactivation components of both channel types: $I(t)/I_{PEAK} = A_{WT}\exp(-t/\tau_{h1WT}) + A_{MT}\exp(-t/\tau_{h1MT}) + A_2\exp(-t/\tau_{h2}) + I_{SS}/I_{PEAK}$ (where WT = wild type and MT =

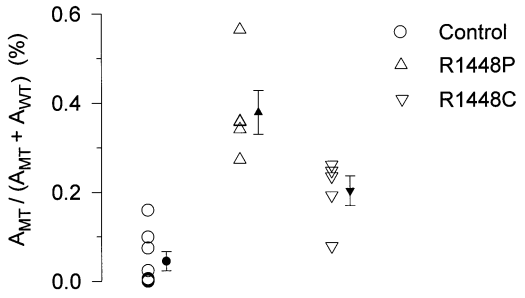

Fig. 4 Relative percentage of mutant channels in paramyotonia congenita muscle specimens. The decay of Na^+ currents recorded in muscle from two paramyotonia congenita patients carrying either the R1448P or the R1448C mutation was fitted to a third-order exponential function: $I(t)/I_{PEAK} = A_{WT} \exp(-t/\tau_{h1WT}) + A_{MT} \exp(-t/\tau_{h1MT}) + A_2 \exp(-t/\tau_{h2}) + I_{SS}/I_{PEAK}$, where A_{WT} and τ_{h1WT} represent the relative amplitude and fast inactivation time constant of wild type channels, respectively, A_{MT} and τ_{h1MT} the relative amplitude and fast inactivation time constant of the mutant channels, A_2 and τ_{h2} the slow component of fast inactivation of both wild-type and mutant channels, and I_{SS}/I_{PEAK} the relative persistent current. The figure shows the relative amplitude $A_{MT}/(A_{MT} + A_{WT})$, representing the estimated number of mutant channels in the paramyotonic muscle specimens. Each symbol represents the result obtained from a single patch; the small, filled symbols with error bars show mean ± SEM for control and both paramyotonic muscles (n = 5–8).

mutant). For accurate separation of the wild-type and mutant time constants and determination of all relative amplitudes, we kept τ_{h1WT} fixed at the average value found for control muscle (0.57 ms) and τ_{h2} at the value obtained from a monoexponential fit of the slowly decaying part of the current (15–45 ms after onset of the depolarization). The values of τ_{h1MT} and all amplitudes were left as free parameters. With these settings, τ_{h1MT} for R1448P channels was 2.25 ± 0.17 ms with a relative amplitude $A_{1MT}/(A_{1WT} + A_{1MT})$ of 38 ± 5% (n = 5). When we repeated the fit using the fixed value of τ_{h1MT} = 2.77 ms obtained from R1448P channels expressed in HEK cells, the result was similar (35 ± 3% mutant channels). When the currents of control muscle were fitted in the same way, $A_{1MT}/(A_{1WT} + A_{1MT})$ was negligibly small (4 ± 2%, n = 8, τ_{h2} = 3.09 ± 0.68 ms).

For a different biopsied muscle specimen from a patient with a moderate form of paramyotonia congenita carrying the R1448C mutation (Becker, 1970), we analysed the current decay using the same fitting procedure as described above. The relative proportion of R1448C channels $A_{1MT}/(A_{1WT} + A_{1MT})$ was determined to be even smaller than for R1448P (only 19.5 ± 1.6%), with a time constant for the mutant channels of τ_{h1MT} = 1.71 ± 10.18 ms (n = 5). The relative amplitudes for all patches recorded from both paramyotonia congenita muscles and normal controls are summarized in Fig. 4. Using this third-order exponential fit, the third time constant was similar for control and both paramyotonia congenita muscles, and generally had a small amplitude [τ_{h2}, 12.4 ± 2.7 (wild type) versus 11.3 ± 1.8 (R1448P) and 12.0 ± 1.8 (R1448C) ms; A_2, 6.3 ± 1.7 versus 6.3 ± 4.0 and 3.0 ± 1.3%]. We therefore conclude that this slow time constant did not significantly disturb our analysis.

For the R1448P mutation, the drastic difference in τ_{h1} ensured a good separation of wild-type and mutant fast inactivation time constants in the paramyotonia congenita muscle specimen. We could clearly separate three time constants of inactivation, whereas in control muscle the relative weight of the second time constant designated to detect mutant channels (τ_{h1MT}) was negligible. For the R1448C mutation, the result of 20% mutant channels is less reliable because of the smaller inactivation defect (only 3-fold increase in τ_{h1}), hence the difficulty in clearly separating the time constants from wild-type and mutant channels. The steady-state inactivation curve for the R1448C mutation measured in HEK cells was shifted by –18 mV compared with wild type ($V_{0.5}$ = –61.5 ± 1.2 and –79.2 ± 2.4 mV; k = 6.1 ± 0.1 and 11.4 ± 0.3 mV; n = 8), and in the paramyotonia congenita muscle containing this mutation this shift was –11.5 mV ($V_{0.5}$ = –93.7 ± 0.4 and –105.2 ± 2.2 mV; k = 8.4 ± 0.3 and 9.3 ± 0.3 mV; n = 5–12). However, it was not possible to separate both mutant and wild-type channels by fitting the inactivation curves to the sum of two Boltzmann functions in paramyotonia congenita muscle from both patients.

A reason for an underestimation of the percentage of mutant channels could be that a higher proportion of mutant channels is inactivated at the prepulse potential of –140 mV. We therefore tested prepulses of up to –160 mV, and could not find a difference in the current decay (results not shown). A prepulse value of –160 mV should be sufficient to let all channels recover from fast inactivation within 300 ms, which was the duration of the prepulse. Since slow inactivation was not significantly different for wild-type and R1448C channels (N. Mitrovic, unpublished results), the holding potential of –100 mV should not have influenced our analysis.

Altogether, we think that our method reliably estimated the percentage of mutant channels in paramyotonia congenita muscle containing the R1448P mutation due to the large difference in τ_{h1}, which enabled a clear separation of mutant and wild-type channels. The 20% share calculated for R1448C channels could be an underestimate since the difference in τ_{h1} was only threefold. Nevertheless, in both cases the proportion of mutant channels was clearly smaller than 50%, as expected from the dominant mode of inheritance.

Using a kinetic analysis of Na^+ currents, we were able to estimate the percentage of functional mutant protein in diseased muscle, a parameter so far unknown in the pathophysiology of channelopathies and other dominantly inherited diseases. In contrast to mRNA measurements, western blots, antibody staining and other molecular biological and biochemical approaches, which determine the level of mutant RNA or protein without regard to its function, the electrophysiogical evaluation allowed us to determine the ratio of the mutant protein that is pathophysiologically relevant. The reduced percentage of mutant channels may have several reasons. The mutated gene could be less expressed or the translation could be

reduced. Also, glycolysation of the protein could be impaired or its incorporation in the membrane could be impeded. In any case, a share of the mutant channels smaller than 50% should reduce the severity of the clinical phenotype. For another Na^+ channelopathy, the equine periodic paralysis in Quarter horses, the severity of the clinical phenotype has been shown to correspond to mRNA levels in native muscle probes (Zhou *et al.*, 1994).

The phenotype of our patient carrying the R1448P mutation is severe (Wang *et al.*, 1995; Lerche *et al.*, 1996), while the phenotype of the other patient is moderate [kinship Q, patient V/26 in Becker (Becker, 1970); Haass *et al.*, 1981]. This was also verified by recent clinical examinations in Ulm. Both patients showed paradoxical myotonia at room temperature, and muscle stiffness upon cooling in ice-cold water followed by weakness lasting up to an hour. The myotonic features were much more pronounced for the patient carrying the R1448P mutation. The gait of this patient was never normal. She walked on her toes and complained about pain in her calves (Wang *et al.*, 1995; Lerche *et al.*, 1996). In the case of the patient carrying the R1448C mutation, the less severe myotonic phenotype could be explained by both the smaller inactivation defect and a reduced number of mutant channels. However, we would like to mention that the R1448C mutation may also cause a severe phenotype in other patients. A possible explanation for this discrepancy may be a higher percentage of mutant channels in these patients.

Although the R1448C patient experiences less severe myotonic symptoms, he suffers from episodes of weakness in a warm environment, similar to patients with hyperkalaemic periodic paralysis, which has not been reported for the R1448P patient. This is in accordance with our hypothesis that weakness is favoured by a hyperpolarizing shift of the steady-state inactivation curve (Lerche *et al.*, 1996; Wagner *et al.*, 1997), which is clearly more pronounced for R1448C than for R1448P channels.

In summary, our data raise the possibility that the clinical phenotype of paramyotonia congenita depends not only on the degree of abnormality of the current conducted by the mutant channels but also on their fraction in the membrane.

Acknowledgements

We wish to thank Drs R. Horn and A. C. Ludolph for helpful discussion, Dr R. Bohlen for collaboration and U. Pika-Hartlaub for performing expert cell culture. This study was supported by the Deutsche Forschungsgemeinschaft (Le481/3), the Muscular Dystrophy Association and the National Institutes of Health (NS32387).

References

Becker PE. Paramyotonia congenita (Eulenburg). Fortschritte der allgemeinen und klinischen Humangenetik, III. Stuttgart: Thieme; 1970.

Catterall WA. Structure and function of voltage-gated ion channels. [Review]. Annu Rev Biochem 1995; 64: 493–531.

Chahine M, George AL Jr, Zhou M, Ji S, Sun W, Barchi RL, et al. Na^+ channel mutations in paramyotonia congenita uncouple inactivation from activation. Neuron 1994; 12: 281–94.

Chen LQ, Santarelli V, Horn R, Kallen RG. A unique role for the S4 segment of domain 4 in the inactivation of sodium channels. J Gen Physiol 1996; 108: 549–56.

Fahlke C, Rüdel R. Giga-seal formation alters properties of sodium channels of human myoballs. Pflugers Arch 1992; 420: 248–54.

Featherstone DE, Fujimoto E, Ruben PC. A defect in skeletal muscle sodium channel deactivation exacerbates hyperexcitability in human paramyotonia congenita. J Physiol (Lond) 1998; 506: 627–38.

Fleischhauer R, Mitrovic N, Deymeer F, Lehmann-Horn F, Lerche H. Effects of temperature and mexiletine on the F1473S Na^+ channel mutation causing paramyotonia congenita. Pflugers Arch 1998; 436: 757–65.

Haass A, Ricker K, Rüdel R, Lehmann-Horn F, Böhlen R, Dengler R, et al. Clinical study of paramyotonia congenita with and without myotonia in a warm environment. Muscle Nerve 1981; 4: 388–95.

Hayward LJ, Brown RH Jr, Cannon SC. Inactivation defects caused by myotonia-associated mutations in the sodium channel III-IV linker. J Gen Physiol 1996; 107: 559–76.

Horn R. Explorations of voltage-dependent conformational changes using cysteine scanning. In: Methods in enzymology. Vol. ? Ion channels. New York: Academic Press. In press 1999.

Lehmann-Horn F, Rüdel R, Ricker R. Membrane defects in paramyotonia congenita (Eulenburg). Muscle Nerve 1987; 10: 633–41.

Lehmann-Horn F, Rüdel R. Molecular pathophysiology of voltage-gated ion channels. [Review]. Rev Physiol Biochem Pharmacol 1996; 128: 195–268.

Lerche H, Mitrovic N, Dubowitz V, Lehmann-Horn F. Paramyotonia congenita: the R1448P Na^+ channel mutation in adult human skeletal muscle. Ann Neurol 1996; 39: 599–608.

Mitrovic N, George AL Jr, Heine R, Wagner S, Pika U, Hartlaub U, et al. K^+-aggravated myotonia: destabilization of the inactivated state of the human muscle Na^+ channel by the V1589M mutation. J Physiol (Lond) 1994; 478: 395–402.

Mitrovic N, George AL Jr, Lerche H, Wagner S, Fahlke C, Lehmann-Horn F. Different effects on gating of three myotonia-causing mutations in the inactivation gate of the human muscle sodium channel. J Physiol (Lond) 1995; 487: 107–14.

Mitrovic N, George AL Jr, Horn R. Independent versus coupled inactivation in sodium channels. Role of the domain 2 S4 segment. J Gen Physiol 1998; 111: 451–62.

Stühmer W, Conti F, Suzuki H, Wang XD, Noda M, Yahagi N, et al. Structural parts involved in activation and inactivation of the sodium channel. Nature 1989; 339: 597–603.

Yang N, Ji S, Zhou M, Ptacek LJ, Barchi RL, Horn R, et al. Sodium channel mutations in paramyotonia congenita exhibit similar biophysical phenotypes in vitro. Proc Natl Acad Sci USA 1994; 91: 12785–9.

Yang N, George AL Jr, Horn R. Molecular basis of charge movement in voltage gated Na^+ channels. Neuron 1996; 16: 113–22.

Wagner S, Lerche H, Mitrovic N, Heine R, George AL, Lehmann-Horn F. A novel sodium channel mutation causing a hyperkalaemic paralytic and paramyotonic syndrome with variable clinical expressivity. Neurology 1997; 49: 1018–25.

Wang J, Dubowitz V, Lehmann-Horn F, Ricker K, Ptacek L, Hoffman EP. In vivo sodium channel structure/function studies: consecutive Arg1448 changes to Cys, His, and Pro at the extracellular surface of IVS4. [Review]. Soc Gen Physiol Ser 1995; 50: 77–88.

Zhou J, Spier SJ, Beech J, Hoffman EP. Pathophysiology of sodium channelopathies: correlation of normal/mutant mRNA ratios with clinical phenotype in dominantly inherited periodic paralysis. Hum Mol Genet 1994; 3: 1599–603.

Received June 25, 1998. Revised January 11, 1999.
Accepted February 1, 1999